

Title

Assessing functional connectivity differences and work-related fatigue in surviving COVID-negative patients.

Running title

Functional Alterations and Fatigue in COVID

Author Names and Affiliations

Rakibul Hafiz ^{‡1}, Tapan Kumar Gandhi^{‡2}, Sapna Mishra², Alok Prasad³, Vidur Mahajan⁴, Benjamin H. Natelson⁵, Xin Di¹, Bharat B. Biswal^{*1}

¹: Department of Biomedical Engineering, New Jersey Institute of Technology (NJIT), 323 Dr Martin Luther King Jr Blvd, Newark, NJ 07102, USA

²: Department of Electrical Engineering, Indian Institute of Technology (IIT), Block II, IIT Delhi Main Rd, IIT Campus, Hauz Khas, New Delhi, Delhi 110016, India

³: Internal Medicine, Irene Hospital & Senior Consultant Medicine, Metro Heart and Super-specialty Hospital, New Delhi, India

⁴: Centre for Advanced Research in Imaging, Neuroscience & Genomics, Mahajan Imaging, New Delhi, India

⁵: Pain and Fatigue Study Center, Department of Neurology, Icahn School of Medicine at Mount Sinai, NY, USA

[‡]: The authors contributed equally for this project as first authors.

* Corresponding Author e-mail

bharat.biswal@njit.edu

Number of pages: 17

Number of figures: 3

Number of Words

Abstract: 176

Introduction: 1103

Discussion: 868

Conflict of interest statement: The authors declare no competing financial interests.

Acknowledgements: This study was supported by an NIH grant (R01AT009829).

1 **Abstract**

2 The recent Coronavirus Disease 2019 (COVID-19) has affected all aspects of life around
3 the world. Neuroimaging evidence suggests the novel coronavirus can attack the central
4 nervous system (CNS), causing cerebro-vascular abnormalities in the brain. This can lead
5 to focal changes in cerebral blood flow and metabolic oxygen consumption rate in the
6 brain. However, the extent and spatial locations of brain alterations in COVID-19 survivors
7 are largely unknown. In this study, we have assessed brain functional connectivity (FC)
8 using resting-state functional MRI (RS-fMRI) in 38 (25 males) COVID patients two weeks
9 after hospital discharge, when PCR negative and 31 (24 males) healthy subjects. FC was
10 estimated using independent component analysis (ICA) and dual regression. The COVID
11 group demonstrated significantly enhanced FC in regions from the Occipital and Parietal
12 Lobes, comparing to the HC group. On the other hand, the COVID group exhibited
13 significantly reduced FC in several vermal layers of the cerebellum. More importantly, we
14 noticed negative correlation of FC with self-reported fatigue within regions from the
15 Parietal lobe, which are known to be associated with fatigue.

16 **Keywords:** *COVID, Functional Connectivity, ICA, Fatigue, RS-fMRI*

17 **Significance Statement**

18 Early neuroimaging studies have mostly focused on structural MRI imaging to report brain
19 abnormalities in acutely ill COVID-19 patients. It is not clear whether functional
20 abnormalities co-exist with structural alterations in patients who have survived the
21 infection and have been discharged from the hospital. A few recent studies have emerged
22 which attempted to address the structural/functional alterations. However, further

23 investigations across different sites are necessary for more conclusive inference. More
24 importantly, fatigue is a highly prevalent symptom among COVID survivors, therefore, the
25 relations of brain imaging abnormalities to fatigue should be investigated. In this study,
26 we try to address these gaps, by collecting imaging data from COVID survivors, now PCR
27 negative, and healthy subjects from a single site – the Indian Institute of Technology (IIT),
28 Delhi, India. Furthermore, this is a continuation of an ongoing study. We have already
29 submitted a manuscript showing structural abnormalities and gray matter volume
30 correlates of self-reported fatigue among this group of COVID survivors.

31 **Introduction**

32 The novel coronavirus pandemic has taken more than 4.5 million lives across the globe
33 ((WHO), 2020). With efforts of vaccination, mask mandates and social distancing, the
34 spread of this contagious disease has been mitigated significantly, however, advents of
35 new strains such as the delta and omicron variants have been setting back progress and
36 especially affecting densely populated countries (India, being a prime example). While
37 the initial wave demanded most medical attention towards severe damage to the
38 respiratory system, recent evidence suggests the novel coronavirus, Severe Acute
39 Respiratory Syndrome Coronavirus 2 (SARS-CoV-2) can also attack the central nervous
40 system (CNS). Early pandemic MRI reports from acutely ill patients show evidence of a
41 wide range of cerebrovascular abnormalities. A review featuring 22 articles (n = 126
42 patients) from seven countries (Gulko et al., 2020) showed that patients with SARS-CoV-
43 2 infection showed acute infarcts, posterior reversible encephalopathy syndrome,
44 hyperintensities from fluid-attenuated inversion recovery (FLAIR) images and

45 microhemorrhages. Another multicenter study (n = 64) also reported higher rates of
46 ischemic strokes (27%) and encephalitis (13%). Moreover, inflammatory vascular
47 pathologies (Keller et al., 2020) and other cerebrovascular abnormalities (Nicholson et
48 al., 2020) have also been reported. Abnormal FLAIR uptakes were also reported in the
49 parietal and occipital lobes among others (Kandemirli et al., 2020), as well as in the
50 hypothalamus and the thalamus in individual patients (Paterson et al., 2020).

51 These single-case reports played a vital role in informing and shaping recent studies with
52 primary focus on group level structural differences in moderate (Duan et al., 2021; Qin et
53 al., 2021) to large sample groups (Douaud et al., 2021). Understandably, the initial target
54 of most neuroimaging studies was brain abnormalities in severe patients. Therefore, a
55 large sample of hospitalized survivors were not investigated, especially those with
56 persistent symptoms. This led to a rise in follow-up studies on a span of 3 to 6 months
57 after initial infection (Lu et al., 2020; Tu et al., 2021) and longitudinal designs (Douaud et
58 al., 2021) where structural abnormalities were investigated before and after the pandemic.
59 We have recently shown gray matter volume differences in survivors after a shorter
60 interval (2 weeks after hospital discharge), as well as, a relation between gray matter
61 volume and self-reported fatigue at work (Hafiz et al., 2021) (in press). It is still unclear,
62 though, if such structural abnormalities are also accompanied by functional brain
63 alterations in COVID-19 survivors.

64 To address this gap, functional brain imaging can be incorporated through functional
65 magnetic resonance imaging (fMRI). Among the earliest literature, a task-based fMRI
66 study reported loss in task activation in the orbito-frontal cortex (OFC) and strong BOLD
67 activations in the piriform cortex (Ismail & Gad, 2021) from a single female (25 years)

68 COVID patient with persistent olfactory dysfunction. They used a simple smell on/off
69 block design task. A single case resting state fMRI (RS-fMRI) study from an
70 unresponsive patient reported intact functional connectivity (FC) of the default mode
71 network (DMN) (Fischer et al., 2020), which was a good prognosis for ultimate recovery.
72 However, these studies were case reports, which leaves the question of whether there
73 are generalizable group level functional brain alterations in COVID survivors. To that
74 end, a few studies have emerged that report various functional abnormalities among
75 COVID survivors. For example, the initial case report from (Fischer et al., 2020) has
76 now been followed up with a group level report with specific focus on severe patients
77 who were initially unresponsive, but recovered completely and were able to return
78 (Fischer et al., 2021) to pre-COVID level behaviorally. When they compared the
79 functional connectivity of these unresponsive patients with healthy controls, they found
80 significantly reduced default mode network (DMN) connectivity and reduction in inter-
81 network connectivity between DMN and salience (SAL) networks. Currently, a growing
82 concern among survivors is persistence of a sequela of symptoms (Logue et al., 2021;
83 Peluso et al., 2021; Tabacof et al., 2020), now commonly called 'Long COVID', which
84 point to brain as the responsible organ. Fatigue, lack of attention, anxiety, memory loss,
85 delayed recovery of smell and/or taste, muscle pain and stress are some of the
86 commonly reported symptoms among many others.

87 Since several of these symptoms suggest cognitive abnormalities among survivors,
88 most contemporary neuroimaging studies have turned their attention to behavioral
89 correlates of functional brain alterations, primarily, post-traumatic stress syndromes
90 (Benedetti et al., 2021; Fu et al., 2021). On the other hand, several others have

91 attempted to use functional connectivity (FC) as a neurobiological indicator of higher
92 stress levels (Liu et al., 2021; Perica et al., 2021), depression (Zhang et al., 2022) and
93 negative affect (Xiao et al., 2021) among only healthy subjects before and after the
94 pandemic.

95 Despite fatigue being one of the most frequently reported symptoms, very little is known
96 of functional brain correlates of fatigue within survivors. Prior to the current study, we
97 have shown a positive correlation of gray matter volume within regions from the *ventral*
98 *basal ganglia (BG)* and *ventromedial prefrontal cortex (vmPFC)* with self-reported
99 fatigue at work in survivors two weeks after hospital discharge (Hafiz et al., 2021) (in
100 press). Here, we continue our investigation to explore the functional correlates of fatigue
101 among the same set of survivors. Moreover, functional changes can occur across
102 different networks among survivors, owing to a range of symptoms experienced during
103 the recovery phase. Therefore, we applied a data driven approach to estimate FC
104 differences between healthy controls (HCs) and surviving, now COVID-negative,
105 patients using RS-fMRI.

106 The earliest 'resting state' study was done by Biswal et al., in 1995 (Biswal et al., 1995),
107 and subsequent studies have shown that spatially distinct regions that are temporally
108 synchronized may share information with each other (Cole et al., 2010; De Luca et al.,
109 2006; Fox et al., 2005; Fox et al., 2006; Greicius et al., 2003; Kalcher et al., 2012; Meier
110 et al., 2012). Independent Component Analysis (ICA), is a data driven technique which
111 groups all voxels in the brain into distinct spatial networks based on the similarity of time
112 courses (McKeown et al., 1998). The large-scale resting-state networks (RSNs) derived
113 from ICA have been shown to have local and higher level associative hierarchy (Yeo et

114 al., 2011) and replicate highly reproducible activation maps across subjects (Smith et al.,
115 2009). FC estimates from group ICA and dual regression (C.F. Beckmann, 2009; Filippini
116 et al., 2009) were used to test our hypothesis that surviving COVID-negative patients
117 would demonstrate altered FC in RSNs comprising of cortical regions where
118 hyperintensities have been reported from single cases and group level differences
119 identified from recent neuroimaging studies. We further hypothesized that FC would
120 demonstrate significant correlation with self-reported fatigue scores in brain regions,
121 known to be associated with fatigue.

122 **Materials and Methods**

123 **Participants**

124 This is a continuation of our recent publication using the same sample groups where
125 structural brain alterations were reported (Hafiz et al., 2021). 47 COVID patients and 35
126 healthy controls were recruited from a single site located at Indian Institute of Technology
127 (IIT), Delhi, India. 9 COVID and 4 HC subjects were removed during quality control and
128 motion assessment, leaving with an effective sample of 38 (25 males) COVID and 31 (24
129 males) HC. The mean age of the COVID group was 34.79 years (SD = ± 10.41 years);
130 and 32.68 years (SD = ± 9.78 years) for the HC group. The COVID subjects were
131 scanned two weeks after they were released from the hospital when confirmed to be
132 COVID-negative upon polymerase chain reaction (PCR) retesting. During scanning, all
133 protocols were strictly followed based on the Institutional Review Board (IRB) guidelines
134 at the Indian Institute of Technology (IIT), Delhi, India.

135 **Clinical Assessment**

136 The most frequently observed symptoms from the participants during hospitalization were
137 - fever, cough, body ache, chills, difficulty breathing, bowel irritation, nausea, loss of
138 sense of smell and loss of consciousness. From the day of discharge till the day of scan,
139 we further asked if the participants were experiencing any persistent or new symptoms.
140 Work-related fatigue (65.6%), muscle pain (50%), lack of sleep (50%), lack of attention
141 (43.8%), headache (40.6%), joint pain (40.6%), memory loss (28.1%), delayed recovery
142 of sense of smell (39%) and/or taste (31%), bowel irritation (33%) and interestingly, hair
143 loss (66%) were commonly reported. Please note, most survivors experienced multiple
144 symptoms simultaneously, hence the ‘%’ represents symptoms that overlap within
145 participants. For example, 43.8% of 27 post-COVID participants reporting with lack of
146 attention also reported a work-related fatigue score > 2 on a scale of 0 to 5, with 0
147 representing no fatigue and 5 representing the highest fatigue possible. The average
148 fatigue score in this sub-set of COVID participants was $2.93/5 \pm 1.21$ [SD].

149 **Brain Imaging**

150 **Anatomical MRI** – High-resolution T1-weighted images were acquired on a 3T GE
151 scanner with a 32-channel head coil in 3D imaging mode with a fast BRAVO sequence.
152 The imaging parameters were TI = 450 ms; 244 x 200 matrix; Flip angle = 12 and FOV =
153 256 mm. The subject was placed in a supine position and the whole brain was scanned
154 in the sagittal configuration where 152 slices were collected, and each slice was 1.00 mm
155 thick. The spatial resolution of all the anatomical scans was 1.0 mm x 1.0 mm x 1.0 mm.

156 **Resting-state fMRI** – A gradient echo planar imaging (EPI) was used to obtain 200
157 whole-brain functional volumes. The parameters were: TR = 2000 ms; TE = 30 ms; Flip
158 angle = 90, 38 slices, matrix = 64x64; FOV = 240 x 240 mm²; acquisition voxel size =
159 3.75 x 3.75 x 3 mm³. The participant was requested to stay as still and motionless as
160 possible with eyes fixed to a cross on an overhead screen.

161 **Data Pre-Processing**

162 The data preprocessing was performed primarily using Statistical Parametric Mapping 12
163 (SPM12) toolbox (<http://www.fil.ion.ucl.ac.uk/spm/>) within a MATLAB environment (The
164 MathWorks, Inc., Natick, MA, USA). However, some steps utilized useful tools from FSL
165 (FMRIB Analysis Group, Oxford, UK) and AFNI (<http://afni.nimh.nih.gov/afni>) (Cox, 1996)
166 for housekeeping, visual inspection and quality control purposes. At the beginning, first
167 five time points were excluded from each subject to account for magnetic stabilization.
168 The functional images were motion corrected for head movement using a least squared
169 approach and 6 parameters (rigid body) spatial transformation with respect to the mean
170 image of the scan. The subjects with excessive head motion were identified using
171 framewise displacement (FWD) (Power et al., 2012). Additionally, time frames with high
172 FWD crossing a threshold of 0.5 mm (Power et al., 2012) were identified along with the
173 previous and the next two frames and added as regressors (Yan et al., 2016) during
174 temporal regression of nuisance signals. If more than 50% of the time series data were
175 affected due to regression of high motion frames the participant was removed from the
176 analysis. Moreover, any participant with the maximum framewise translation or rotation
177 exceeding 2 mm was removed from further analysis. Anatomical image from each subject
178 was coregistered to the mean functional image obtained from the motion correction step.

179 T1-weighted image from each subject was segmented into gray matter (GM), white matter
180 (WM), and cerebrospinal fluid (CSF) tissue probability maps and an average template
181 including all participants was generated using DARTEL (Ashburner, 2007). This template
182 was used to spatially normalize all functional images to the MNI space and resampled to
183 isotropic voxel size of 3 mm x 3 mm x 3 mm. Time series, from brain compartments with
184 high physiological noise signals such as, CSF and WM was extracted by thresholding the
185 probability maps from the segmentation stage above the 99th percentile, and first 5
186 principal components were obtained using a COMPCOR based (Behzadi et al., 2007)
187 principal component analysis (PCA) from both tissues. These 10 components along with
188 Friston's 24- parameter model (6 head motion parameters + 6 previous time point motion
189 parameters + 12 corresponding quadratic parameters) (Friston et al., 1996) and time
190 frames with high FWD (> 0.5 mm) were added as regressors in a multiple linear
191 regression model to remove unwanted signals voxel-wise. The residuals from the
192 regression step were then bandpass filtered between 0.01 to 0.1 Hz and finally, spatial
193 smoothing was performed using a Gaussian kernel of 6 mm full width at half maximum
194 (FWHM).

195 **Head Motion Assessment**

196 We performed in-scanner head movement assessment using mean Framewise
197 Displacement (FWD) based on the methods depicted in (Power et al., 2012). A two-tailed
198 two-sample student's t-test revealed no significant differences in mean FWD between the
199 two groups ($t = -1.57$, $p = 0.12$, $\alpha = 0.05$).

200 **ICA and Dual Regression**

201 Group level resting state networks were obtained by applying the ‘gica’ option of the
202 ‘melodic’ module from FSL toolbox (FMRIB Analysis Group, Oxford, UK). All subjects’ 4D
203 functional images after pre-processing were temporally concatenated into a 2D matrix of
204 ‘space’ x ‘time’ as delineated in (C.F. Beckmann, 2009) and 25 spatial maps were
205 obtained. Resting State Networks (RSNs) were identified by matching ICs with the 1000
206 functional connectome project maps (Biswal et al., 2010) using Dice’s coefficient and
207 spatial correlations obtained from AFNI’s ‘3dMatch’ program (Taylor & Saad, 2013).
208 Further visual inspection was performed to make sure all network regions aligned with
209 the functional network and ROIs depicted in (Altmann et al., 2015; Shirer et al., 2012).
210 Dual regression (C.F. Beckmann, 2009; Filippini et al., 2009) was performed leveraging
211 the standardized group ICA output from the ‘melodic’ step and applying it directly to the
212 ‘fsl-glm’ module in FSL to obtain subject specific RSN maps. The subject specific network
213 maps were standardized to Z-scores before consequently applying them in statistical
214 analysis to infer group level estimates.

215 **Statistical Analysis**

216 To investigate FC differences between COVID and HC groups, we performed an unpaired
217 two sample t-test between standardized subject-specific RSN maps from the two groups.
218 Significant clusters were identified and main effect of interest from the corresponding
219 contrast maps representing the difference in mean beta scores from two groups were
220 obtained by thresholding the t-score map values that survived the corrected threshold. To
221 account for confounding effects that may explain some of the variance in the data, age
222 and sex were also added as covariates of no interest. Cluster-based thresholding was

223 applied at height threshold of $p_{unc} < 0.01$, with *family wise error (FWE)* correction at p_{FWE}
224 < 0.05 for multiple comparisons. The cluster extent threshold (k_E) obtained from this step
225 was used to generate corrected statistical maps for the contrasts with significant effects.

226 We further wanted to evaluate which of the large scale RSNs demonstrates linear
227 relationship or correlation with self-reported fatigue among the COVID individuals. We
228 incorporated a multiple linear regression approach where the FC at each voxel was the
229 response variable (Y), and the self-reported fatigue score was the explanatory variable
230 (X). We also added age and sex as covariates of no interest. Significant clusters were
231 obtained in the same manner as described earlier in this section for group level
232 differences in FC. For visual representation of the significant linear relationship between
233 the two variables, the average FC within the significant cluster was obtained from each
234 subject. These average FC values were then linearly regressed against the fatigue scores
235 and visualized within a scatter plot and a line of best fit with 95% confidence interval. Age
236 and sex were regressed out during the linear regression step. The correlation analysis
237 and the graphical plotting was done using 'inhouse' scripts prepared in RStudio (RStudio,
238 2021).

239 **Results**

240

241 We identified twenty-two large-scale resting state networks (RSNs) (see Figure1) from
242 the group ICA analysis. Group level statistical analysis was run for each network using
243 standardized subject specific RSN maps obtained from the dual regression step.
244 Significantly enhanced FC was observed in the COVID group compared to the HC group

245 in particularly regions from the *occipital* and *parietal* lobes. Figures 2 and 3 show all
246 significant clusters from the FC and linear regression analysis, respectively.

247 Figure 2 shows the results from the group level analysis from three RSNs. Figure 2 A (top
248 row) demonstrates regions with significantly enhanced FC in the COVID-19 group
249 compared to the HC group for the *BGN* network. The FC difference was observed in the
250 *Right – Calcarine Cortex (Calc)*, *Cuneus (Cu)* and *Lingual Gyrus (LiG)* regions of the
251 *occipital* lobe. Similarly, the COVID survivors also demonstrated enhanced FC of the *PRN*
252 network (Figure 2 B) with regions from the *Parietal Lobe: Bilateral – Superior Parietal*
253 *Lobule (SPL)* and *Precuneus (PCu)* regions. On the other hand, Figure 2 C shows reduced
254 functional connectivity among COVID participants compared to HCs in several layers of
255 the *cerebellar vermal lobules (CVL) (I-V, VI-VII)* for the *LANG* network. The cluster peak
256 information including peak T-scores and *FWE* corrected exact p-values with relevant
257 spatial regions from each network showing significant differences have been tabulated
258 for an easy reference in Table 1.

259 Figure 3 shows brain regions where a significant negative correlation was observed
260 between FC and self-reported fatigue, from the *PRN* network. Figure 3 (A) (left) shows the
261 cluster where a negative correlation between FC and fatigue scores was observed in the
262 *Left – Superior Parietal Lobule (SPL)*, *Superior Occipital Gyrus (SOG)*, *Angular Gyrus*
263 *(AnG)* and *Precuneus (PCu)*. The graph on the right visually presents this negative

264 relationship ($r = -0.75$, $p = 0.00001$, $r^2 = 0.56$) between the average FC of this cluster and
265 fatigue scores.

266

267 **Discussion**

268 The results from this study support our hypothesis that COVID survivors would
269 demonstrate altered FC when compared to HCs, even two weeks after discharge from
270 the hospital and demonstrate significant linear relationship with work-related fatigue. Our
271 hypothesis was based on both early case-reports and more recent group level
272 neuroimaging reports of structural and functional brain alterations. Individual case reports
273 were primarily from acutely ill patients using FLAIR (Kandemirli et al., 2020; Kremer et
274 al., 2020; Paterson et al., 2020) and Susceptibility Weighted Imaging (SWI) (Conklin et
275 al., 2021), whereas, group level reports, such as those derived from fMRI, include,
276 reduced *default mode* and *saliience* connectivity (Fischer et al., 2021) and high prevalence
277 of abnormal time varying and topological organizations between *sensorimotor* and *visual*
278 networks (Fu et al., 2021). In the current context, we report between group FC alterations
279 of three large scale RSNs – *BGN*, *PRN* and *LANG* networks and further show negative
280 correlation of FC from the *PRN* network with self-reported fatigue at work among COVID
281 survivors.

282 While initially a single patient showed no differences in FC of *DMN* when compared to
283 five healthy controls (Fischer et al., 2020), Fischer and colleagues recently reported
284 reduced FC within *DMN* and between *DMN* and *SAL* networks after group level
285 assessment (Fischer et al., 2021). In the current study, we did not observe any significant

286 alterations in posterior or ventral DMN (PDMN and VDMN) networks, but our patient
287 group was not unresponsive and as acutely ill as the patients reported in (Fischer et al.,
288 2021). However, we did observe differences in FC for the PRN network which consists of
289 *Precuneus (PCu)*, *Frontal Eye Fields (FEF)* and parts of the *Superior Parietal Lobule*
290 (*SPL*). Enhanced FC in this network was observed in the *Bilateral SPL* and *PCu* regions.
291 *PCu* is a constituent of DMN, and higher functional connectivity with this region may
292 indicate some compensatory mechanism due to loss in connections in other pathways.
293 Furthermore, *SPL* is a constituent of the *posterior parietal cortex (PPC)* which has been
294 shown to have functional association with altered *anterior insula* connectivity in chronic
295 fatigue syndrome (CFS) (Wortinger et al., 2017). Moreover, these brain regions are also
296 known to be involved in attention processing, therefore, enhanced FC in these regions
297 may indicate possible compensatory mechanisms of attention related symptoms that
298 recovering patients may experience. Therefore, further investigations are necessary to
299 understand these processes better, especially, from a clinical perspective.

300 Enhanced FC in the COVID group was also observed for the *BGN* network within the
301 occipital lobe (*Calc*, *Cu* and *LiG*). *Calc* and *Cu* are primarily involved in visual processing.
302 Fu and colleagues reported that COVID survivors had higher connectivity between
303 *Cerebellum*, *Sensorimotor* and *Visual* networks, indicating they spent abnormally higher
304 time in a specific brain state compared to healthy controls (Fu et al., 2021). A recent study
305 has also suggested *Cu* to be a major hub for mild cognitive impairment in idiopathic REM
306 sleep behavior disorder (iRBD) (Mattioli et al., 2021). *LiG* and weak *insular* coactivation
307 with the *occipital* cortex have been shown to be associated with disrupted salience
308 processing that can lead to loss in motivation in day-to-day tasks (Kim et al., 2018).

309 Moreover, the *basal ganglia* are known to be associated with fatigue (Miller et al., 2014),
310 cognitive, emotional and attention processing (Di Martino et al., 2008; van Schouwenburg
311 et al., 2015). We also observed reduced FC within several layers of the *Cerebellar Vermal*
312 *Lobules* among COVID participants when compared to HCs. These lobules have been
313 suggested to be involved in cognition and emotion processing (Park et al., 2018). The
314 synergy of these studies to our findings indicates possible functional brain associations
315 of commonly observed symptoms in survivors with post-acute sequelae SARS-CoV-2
316 infection (PASC or Long COVID) lasting many months (Carfi et al., 2020; Garrigues et
317 al., 2020; Logue et al., 2021; Peluso et al., 2021). FC alterations in multiple networks also
318 suggest that RS-fMRI can be quite useful to investigate multiple brain networks across
319 the whole brain (Damoiseaux et al., 2006; Raichle & Mintun, 2006; Shulman et al., 2004)
320 in COVID-19 patients. The results also suggest a possible link between structural and
321 functional abnormalities in COVID patients since the FC alterations were observed in
322 regions that align with anatomical regions exhibiting hyperintensities from FLAIR and SWI
323 studies.

324 We further evaluated linear relationship between FC of RSNs and self-reported fatigue at
325 work among COVID participants. We observed a significant negative correlation of FC
326 with fatigue within the *Left SPL*, *SOG*, *AnG* and *PCu*, i.e., brain regions primarily
327 belonging to the *parietal* lobe (see Table2 for cluster information). Structural atrophy in
328 the *parietal* lobe has been shown to be associated with fatigue among multiple sclerosis
329 (MS) patients (Calabrese et al., 2010; Pellicano et al., 2010). An RS-fMRI study of patients
330 with chronic fatigue syndrome (CFS) used ICA to reveal loss of intrinsic connectivity in
331 the parietal lobe (Gay et al., 2016). It is interesting that lower FC in the parietal lobe

332 correlates negatively to higher fatigue scores among COVID survivors. To the best of our
333 knowledge, this is the first study to show work-related fatigue correlates of FC among
334 recovering patients 2 weeks after hospital discharge. Therefore, future studies are
335 necessary to evaluate this avenue further in the surviving cohorts.

336

337 **Limitations**

338 Despite our efforts to show group level effects that reflect individual and group level
339 reports in the recent literature, our study still maintains a cross-sectional design. In cases
340 like this, a better approach for the future would be to use follow up designs (Fu et al.,
341 2021; Lu et al., 2020; Tu et al., 2021) or possibly a longitudinal design where patients
342 could be observed both before and after the pandemic like the one using the UK-biobank
343 (Douaud et al., 2021). Our effort here, was to show group level effects at an early stage
344 of recovery (2 weeks after hospital discharge) and determine the relation between work-
345 related fatigue and FC of RSNs. We believe the results from this study will help
346 understanding the recovery stage brain alterations and how they might drive fatigue-
347 related symptoms among COVID survivors.

348

349 **Author Credit Statement**

350

351 **Rakibul Hafiz:** Methodology, Software, Formal Analysis, Data Curation, Writing –
352 Original Draft, Review and Editing.

353 **Tapan K. Gandhi:** Conceptualization, Investigation, Resources, Supervision, Writing –
354 Review and Editing.

355 **Sapna Mishra:** Investigation, Resources, Data Curation, Writing – Review and Editing.

356 **Alok Prasad:** Writing – Review and Editing.

357 **Vidur Mahajan:** Writing – Review and Editing.

358 **Xin Di:** Methodology, Writing – Review and Editing.

359 **Benjamin H. Natelson:** Writing – Review and Editing.

360 **Bharat Biswal:** Conceptualization, Resources, Project Administration, Supervision,
361 Writing – Review and Editing.

362

363

364

365

366 References

- 367 (WHO), W. H. O. (2020, 10/21/2021, 4:46pm CET). *WHO Coronavirus Disease (COVID-19)*
368 *Dashboard*. Retrieved 10/21/2021 from <https://covid19.who.int/table>
- 369 Altmann, A., Ng, B., Landau, S. M., Jagust, W. J., & Greicius, M. D. (2015). Regional brain
370 hypometabolism is unrelated to regional amyloid plaque burden. *Brain*, *138*(Pt 12),
371 3734-3746. <https://doi.org/10.1093/brain/awv278>
- 372 Ashburner, J. (2007). A fast diffeomorphic image registration algorithm. *Neuroimage*, *38*(1),
373 95-113. <https://doi.org/10.1016/j.neuroimage.2007.07.007>
- 374 Behzadi, Y., Restom, K., Liau, J., & Liu, T. T. (2007). A component based noise correction
375 method (CompCor) for BOLD and perfusion based fMRI. *Neuroimage*, *37*(1), 90-101.
376 <https://doi.org/10.1016/j.neuroimage.2007.04.042>
- 377 Benedetti, F., Palladini, M., Paolini, M., Melloni, E., Vai, B., De Lorenzo, R., Furlan, R., Rovere-
378 Querini, P., Falini, A., & Mazza, M. G. (2021). Brain correlates of depression, post-
379 traumatic distress, and inflammatory biomarkers in COVID-19 survivors: A
380 multimodal magnetic resonance imaging study. *Brain, behavior, & immunity - health*,
381 *18*, 100387-100387. <https://doi.org/10.1016/j.bbih.2021.100387>
- 382 Biswal, B., Yetkin, F. Z., Haughton, V. M., & Hyde, J. S. (1995). Functional connectivity in the
383 motor cortex of resting human brain using echo-planar MRI. *Magn Reson Med*, *34*(4),
384 537-541.
- 385 Biswal, B. B., Mennes, M., Zuo, X.-N., Gohel, S., Kelly, C., Smith, S. M., Beckmann, C. F.,
386 Adelstein, J. S., Buckner, R. L., Colcombe, S., Dogonowski, A.-M., Ernst, M., Fair, D.,
387 Hampson, M., Hoptman, M. J., Hyde, J. S., Kiviniemi, V. J., Kötter, R., Li, S.-J., . . . Milham,
388 M. P. (2010). Toward discovery science of human brain function. *Proceedings of the*
389 *National Academy of Sciences*, *107*(10), 4734-4739.
390 <https://doi.org/10.1073/pnas.0911855107>
- 391 C.F. Beckmann, C. E. M., N. Filippini, and S.M. Smith. (2009). Group comparison of resting-
392 state FMRI data using multi-subject ICA and dual regression. *OHBM*.
- 393 Calabrese, M., Rinaldi, F., Grossi, P., Mattisi, I., Bernardi, V., Favaretto, A., Perini, P., & Gallo,
394 P. (2010). Basal ganglia and frontal/parietal cortical atrophy is associated with
395 fatigue in relapsing-remitting multiple sclerosis. *Mult Scler*, *16*(10), 1220-1228.
396 <https://doi.org/10.1177/1352458510376405>
- 397 Carfi, A., Bernabei, R., Landi, F., & Gemelli Against, C.-P.-A. C. S. G. (2020). Persistent
398 Symptoms in Patients After Acute COVID-19. *JAMA*, *324*(6), 603-605.
399 <https://doi.org/10.1001/jama.2020.12603>
- 400 Cole, D. M., Smith, S. M., & Beckmann, C. F. (2010). Advances and pitfalls in the analysis and
401 interpretation of resting-state FMRI data. *Front Syst Neurosci*, *4*, 8.
402 <https://doi.org/10.3389/fnsys.2010.00008>
- 403 Conklin, J., Frosch, M. P., Mukerji, S. S., Rapalino, O., Maher, M. D., Schaefer, P. W., Lev, M. H.,
404 Gonzalez, R. G., Das, S., Champion, S. N., Magdamo, C., Sen, P., Harrold, G. K., Alabsi, H.,
405 Normandin, E., Shaw, B., Lemieux, J. E., Sabeti, P. C., Branda, J. A., . . . Edlow, B. L.
406 (2021). Susceptibility-weighted imaging reveals cerebral microvascular injury in
407 severe COVID-19. *Journal of the Neurological Sciences*, *421*, 117308-117308.
408 <https://doi.org/10.1016/j.jns.2021.117308>
- 409 Cox, R. W. (1996). AFNI: software for analysis and visualization of functional magnetic
410 resonance neuroimages. *Comput Biomed Res*, *29*(3), 162-173.

- 411 Damoiseaux, J. S., Rombouts, S. A., Barkhof, F., Scheltens, P., Stam, C. J., Smith, S. M., &
412 Beckmann, C. F. (2006). Consistent resting-state networks across healthy subjects.
413 *Proc Natl Acad Sci U S A*, *103*(37), 13848-13853.
414 <https://doi.org/10.1073/pnas.0601417103>
- 415 De Luca, M., Beckmann, C. F., De Stefano, N., Matthews, P. M., & Smith, S. M. (2006). fMRI
416 resting state networks define distinct modes of long-distance interactions in the
417 human brain. *Neuroimage*, *29*(4), 1359-1367.
418 <https://doi.org/10.1016/j.neuroimage.2005.08.035>
- 419 Di Martino, A., Scheres, A., Margulies, D. S., Kelly, A. M., Uddin, L. Q., Shehzad, Z., Biswal, B.,
420 Walters, J. R., Castellanos, F. X., & Milham, M. P. (2008). Functional connectivity of
421 human striatum: a resting state FMRI study. *Cereb Cortex*, *18*(12), 2735-2747.
422 <https://doi.org/10.1093/cercor/bhn041>
- 423 Douaud, G., Lee, S., Alfaro-Almagro, F., Arthofer, C., Wang, C., Lange, F., Andersson, J. L. R.,
424 Griffanti, L., Duff, E., Jbabdi, S., Taschler, B., Winkler, A., Nichols, T. E., Collins, R.,
425 Matthews, P. M., Allen, N., Miller, K. L., & Smith, S. M. (2021). Brain imaging before
426 and after COVID-19 in UK Biobank. *medRxiv*.
427 <https://doi.org/10.1101/2021.06.11.21258690>
- 428 Duan, K., Premi, E., Pilotto, A., Cristillo, V., Benussi, A., Libri, I., Giunta, M., Bockholt, H. J., Liu,
429 J., Campora, R., Pezzini, A., Gasparotti, R., Magoni, M., Padovani, A., & Calhoun, V. D.
430 (2021). Alterations of frontal-temporal gray matter volume associate with clinical
431 measures of older adults with COVID-19. *Neurobiol Stress*, *14*, 100326.
432 <https://doi.org/10.1016/j.ynstr.2021.100326>
- 433 Filippini, N., MacIntosh, B. J., Hough, M. G., Goodwin, G. M., Frisoni, G. B., Smith, S. M.,
434 Matthews, P. M., Beckmann, C. F., & Mackay, C. E. (2009). Distinct patterns of brain
435 activity in young carriers of the APOE-epsilon4 allele. *Proc Natl Acad Sci U S A*,
436 *106*(17), 7209-7214. <https://doi.org/10.1073/pnas.0811879106>
- 437 Fischer, D., Snider, S. B., Barra, M. E., Sanders, W. R., Rapalino, O., Schaefer, P., Foulkes, A. S.,
438 Bodien, Y. G., & Edlow, B. L. (2021). Disorders of Consciousness Associated With
439 COVID-19: A Prospective, Multimodal Study of Recovery and Brain Connectivity.
440 *Neurology*. <https://doi.org/10.1212/wnl.0000000000013067>
- 441 Fischer, D., Threlkeld, Z. D., Bodien, Y. G., Kirsch, J. E., Huang, S. Y., Schaefer, P. W., Rapalino,
442 O., Hochberg, L. R., Rosen, B. R., & Edlow, B. L. (2020). Intact Brain Network Function
443 in an Unresponsive Patient with COVID-19. *Annals of neurology*, *88*(4), 851-854.
444 <https://doi.org/10.1002/ana.25838>
- 445 Fox, M. D., Snyder, A. Z., Vincent, J. L., Corbetta, M., Van Essen, D. C., & Raichle, M. E. (2005).
446 The human brain is intrinsically organized into dynamic, anticorrelated functional
447 networks. *Proc Natl Acad Sci U S A*, *102*(27), 9673-9678.
448 <https://doi.org/10.1073/pnas.0504136102>
- 449 Fox, M. D., Snyder, A. Z., Zacks, J. M., & Raichle, M. E. (2006). Coherent spontaneous activity
450 accounts for trial-to-trial variability in human evoked brain responses. *Nat Neurosci*,
451 *9*(1), 23-25. <https://doi.org/10.1038/nn1616>
- 452 Friston, K. J., Williams, S., Howard, R., Frackowiak, R. S., & Turner, R. (1996). Movement-
453 related effects in fMRI time-series. *Magn Reson Med*, *35*(3), 346-355.
- 454 Fu, Z., Tu, Y., Calhoun, V. D., Zhang, Y., Zhao, Q., Chen, J., Meng, Q., Lu, Z., & Hu, L. (2021).
455 Dynamic functional network connectivity associated with post-traumatic stress

- 456 symptoms in COVID-19 survivors. *Neurobiology of Stress*, *15*, 100377.
457 <https://doi.org/https://doi.org/10.1016/j.ynstr.2021.100377>
- 458 Garrigues, E., Janvier, P., Kherabi, Y., Le Bot, A., Hamon, A., Gouze, H., Doucet, L., Berkani, S.,
459 Oliosi, E., Mallart, E., Corre, F., Zarrouk, V., Moyer, J. D., Galy, A., Honsel, V., Fantin, B.,
460 & Nguyen, Y. (2020). Post-discharge persistent symptoms and health-related quality
461 of life after hospitalization for COVID-19. *J Infect*, *81*(6), e4-e6.
462 <https://doi.org/10.1016/j.jinf.2020.08.029>
- 463 Gay, C. W., Robinson, M. E., Lai, S., O'Shea, A., Craggs, J. G., Price, D. D., & Staud, R. (2016).
464 Abnormal Resting-State Functional Connectivity in Patients with Chronic Fatigue
465 Syndrome: Results of Seed and Data-Driven Analyses. *Brain Connect*, *6*(1), 48-56.
466 <https://doi.org/10.1089/brain.2015.0366>
- 467 Greicius, M. D., Krasnow, B., Reiss, A. L., & Menon, V. (2003). Functional connectivity in the
468 resting brain: a network analysis of the default mode hypothesis. *Proc Natl Acad Sci*
469 *U S A*, *100*(1), 253-258. <https://doi.org/10.1073/pnas.0135058100>
- 470 Gulko, E., Oleksk, M. L., Gomes, W., Ali, S., Mehta, H., Overby, P., Al-Mufti, F., & Rozenshtein,
471 A. (2020). MRI Brain Findings in 126 Patients with COVID-19: Initial Observations
472 from a Descriptive Literature Review. *American Journal of Neuroradiology*.
473 <https://doi.org/10.3174/ajnr.A6805>
- 474 Hafiz, R., Gandhi, T. K., Mishra, S., Prasad, A., Mahajan, V., Di, X., Natelson, B. H., & Biswal, B.
475 B. (2021). Higher Limbic and Basal Ganglia volumes in surviving COVID-negative
476 patients and the relations to fatigue. *medRxiv*, 2021.2011.2023.21266761.
477 <https://doi.org/10.1101/2021.11.23.21266761>
- 478 Ismail, I. I., & Gad, K. A. (2021). Absent Blood Oxygen Level-Dependent Functional Magnetic
479 Resonance Imaging Activation of the Orbitofrontal Cortex in a Patient With
480 Persistent Cacosmia and Cacogeusia After COVID-19 Infection. *JAMA Neurology*.
481 <https://doi.org/10.1001/jamaneurol.2021.0009>
- 482 Kalcher, K., Huf, W., Boubela, R. N., Filzmoser, P., Pezawas, L., Biswal, B., Kasper, S., Moser,
483 E., & Windischberger, C. (2012). Fully exploratory network independent component
484 analysis of the 1000 functional connectomes database. *Front Hum Neurosci*, *6*, 301.
485 <https://doi.org/10.3389/fnhum.2012.00301>
- 486 Kandemirli, S. G., Dogan, L., Sarikaya, Z. T., Kara, S., Akinci, C., Kaya, D., Kaya, Y., Yildirim, D.,
487 Tuzuner, F., Yildirim, M. S., Ozluk, E., Gucyetmez, B., Karaarslan, E., Koyluoglu, I.,
488 Demirel Kaya, H. S., Mammadov, O., Kisa Ozdemir, I., Afsar, N., Citci Yalcinkaya, B., . . .
489 Kocer, N. (2020). Brain MRI Findings in Patients in the Intensive Care Unit with
490 COVID-19 Infection. *Radiology*, *297*(1), E232-e235.
491 <https://doi.org/10.1148/radiol.2020201697>
- 492 Keller, E., Brandi, G., Winklhofer, S., Imbach, L. L., Kirschenbaum, D., Frontzek, K., Steiger, P.,
493 Dietler, S., Haeblerlin, M., Willms, J., Porta, F., Waeckerlin, A., Huber, M., Abela, I. A.,
494 Lutterotti, A., Stippich, C., Globas, C., Varga, Z., & Jelcic, I. (2020). Large and Small
495 Cerebral Vessel Involvement in Severe COVID-19: Detailed Clinical Workup of a Case
496 Series. *Stroke*, *51*(12), 3719-3722. <https://doi.org/10.1161/strokeaha.120.031224>
- 497 Kim, B. H., Shin, Y. B., Kyeong, S., Lee, S. K., & Kim, J. J. (2018). Disrupted salience processing
498 involved in motivational deficits for real-life activities in patients with
499 schizophrenia. *Schizophr Res*, *197*, 407-413.
500 <https://doi.org/10.1016/j.schres.2018.01.019>

- 501 Kremer, S., Lersy, F., Anheim, M., Merdji, H., Schenck, M., Oesterlé, H., Bolognini, F., Messie, J.,
502 Khalil, A., Gaudemer, A., Carré, S., Alleg, M., Lecocq, C., Schmitt, E., Anxionnat, R., Zhu,
503 F., Jager, L., Nesser, P., Mba, Y. T., . . . Cotton, F. (2020). Neurologic and neuroimaging
504 findings in patients with COVID-19: A retrospective multicenter study. *Neurology*,
505 95(13), e1868-e1882. <https://doi.org/10.1212/wnl.0000000000010112>
- 506 Liu, P., Yang, W., Zhuang, K., Wei, D., Yu, R., Huang, X., & Qiu, J. (2021). The functional
507 connectome predicts feeling of stress on regular days and during the COVID-19
508 pandemic. *Neurobiol Stress*, 14, 100285.
509 <https://doi.org/10.1016/j.ynstr.2020.100285>
- 510 Logue, J. K., Franko, N. M., McCulloch, D. J., McDonald, D., Magedson, A., Wolf, C. R., & Chu, H.
511 Y. (2021). Sequelae in Adults at 6 Months After COVID-19 Infection. *JAMA Netw*
512 *Open*, 4(2), e210830. <https://doi.org/10.1001/jamanetworkopen.2021.0830>
- 513 Lu, Y., Li, X., Geng, D., Mei, N., Wu, P.-Y., Huang, C.-C., Jia, T., Zhao, Y., Wang, D., Xiao, A., & Yin,
514 B. (2020). Cerebral Micro-Structural Changes in COVID-19 Patients – An
515 MRI-based 3-month Follow-up Study. *EClinicalMedicine*, 25.
516 <https://doi.org/10.1016/j.eclinm.2020.100484>
- 517 Mattioli, P., Pardini, M., Famà, F., Girtler, N., Brugnolo, A., Orso, B., Meli, R., Filippi, L.,
518 Grisanti, S., Massa, F., Bauckneht, M., Miceli, A., Terzaghi, M., Morbelli, S., Nobili, F., &
519 Arnaldi, D. (2021). Cuneus/precuneus as a central hub for brain functional
520 connectivity of mild cognitive impairment in idiopathic REM sleep behavior
521 patients. *Eur J Nucl Med Mol Imaging*, 48(9), 2834-2845.
522 <https://doi.org/10.1007/s00259-021-05205-6>
- 523 McKeown, M. J., Makeig, S., Brown, G. G., Jung, T. P., Kindermann, S. S., Bell, A. J., & Sejnowski,
524 T. J. (1998). Analysis of fMRI data by blind separation into independent spatial
525 components. *Hum Brain Mapp*, 6(3), 160-188. [https://doi.org/10.1002/\(SICI\)1097-
526 0193\(1998\)6:3<#x0003c;160::AID-HBM5<#x0003e;3.0.CO;2-1](https://doi.org/10.1002/(SICI)1097-0193(1998)6:3<#x0003c;160::AID-HBM5<#x0003e;3.0.CO;2-1)
- 527 Meier, T. B., Wildenberg, J. C., Liu, J., Chen, J., Calhoun, V. D., Biswal, B. B., Meyerand, M. E.,
528 Birn, R. M., & Prabhakaran, V. (2012). Parallel ICA identifies sub-components of
529 resting state networks that covary with behavioral indices. *Front Hum Neurosci*, 6,
530 281. <https://doi.org/10.3389/fnhum.2012.00281>
- 531 Miller, A. H., Jones, J. F., Drake, D. F., Tian, H., Unger, E. R., & Pagnoni, G. (2014). Decreased
532 basal ganglia activation in subjects with chronic fatigue syndrome: association with
533 symptoms of fatigue. *PLoS One*, 9(5), e98156.
534 <https://doi.org/10.1371/journal.pone.0098156>
- 535 Nicholson, P., Alshafai, L., & Krings, T. (2020). Neuroimaging Findings in Patients with
536 COVID-19. *American Journal of Neuroradiology*, 41(8), 1380-1383.
537 <https://doi.org/10.3174/ajnr.A6630>
- 538 Park, I. S., Lee, N. J., & Rhyu, I. J. (2018). Roles of the Declive, Folium, and Tuber Cerebellar
539 Vermian Lobules in Sportspeople. *Journal of clinical neurology (Seoul, Korea)*, 14(1),
540 1-7. <https://doi.org/10.3988/jcn.2018.14.1.1>
- 541 Paterson, R. W., Brown, R. L., Benjamin, L., Nortley, R., Wiethoff, S., Bharucha, T., Jayaseelan,
542 D. L., Kumar, G., Raftopoulos, R. E., Zambreanu, L., Vivekanandam, V., Khoo, A.,
543 Geraldès, R., Chinthapalli, K., Boyd, E., Tuzlali, H., Price, G., Christofi, G., Morrow, J., . . .
544 Zandi, M. S. (2020). The emerging spectrum of COVID-19 neurology: clinical,
545 radiological and laboratory findings. *Brain*, 143(10), 3104-3120.
546 <https://doi.org/10.1093/brain/awaa240>

- 547 Pellicano, C., Gallo, A., Li, X., Ikonomidou, V. N., Evangelou, I. E., Ohayon, J. M., Stern, S. K.,
548 Ehrmantraut, M., Cantor, F., McFarland, H. F., & Bagnato, F. (2010). Relationship of
549 Cortical Atrophy to Fatigue in Patients With Multiple Sclerosis. *Archives of*
550 *Neurology*, 67(4), 447-453. <https://doi.org/10.1001/archneurol.2010.48>
- 551 Peluso, M. J., Kelly, J. D., Lu, S., Goldberg, S. A., Davidson, M. C., Mathur, S., Durstenfeld, M. S.,
552 Spinelli, M. A., Hoh, R., Tai, V., Fehrman, E. A., Torres, L., Hernandez, Y., Williams, M.
553 C., Arreguin, M. I., Bautista, J. A., Ngo, L. H., Deswal, M., Munter, S. E., . . . Martin, J. N.
554 (2021). Rapid implementation of a cohort for the study of post-acute sequelae of
555 SARS-CoV-2 infection/COVID-19. *medRxiv*, 2021.2003.2011.21252311.
556 <https://doi.org/10.1101/2021.03.11.21252311>
- 557 Perica, M. I., Ravindranath, O., Calabro, F. J., Foran, W., & Luna, B. (2021). Hippocampal-
558 Prefrontal Connectivity Prior to the COVID-19 Pandemic Predicts Stress Reactivity.
559 *Biol Psychiatry Glob Open Sci*, 1(4), 283-290.
560 <https://doi.org/10.1016/j.bpsgos.2021.06.010>
- 561 Power, J. D., Barnes, K. A., Snyder, A. Z., Schlaggar, B. L., & Petersen, S. E. (2012). Spurious
562 but systematic correlations in functional connectivity MRI networks arise from
563 subject motion. *Neuroimage*, 59(3), 2142-2154.
564 <https://doi.org/10.1016/j.neuroimage.2011.10.018>
- 565 Qin, Y., Wu, J., Chen, T., Li, J., Zhang, G., Wu, D., Zhou, Y., Zheng, N., Cai, A., Ning, Q., Manyande,
566 A., Xu, F., Wang, J., & Zhu, W. (2021). Long-term microstructure and cerebral blood
567 flow changes in patients recovered from COVID-19 without neurological
568 manifestations. *J Clin Invest*, 131(8). <https://doi.org/10.1172/jci147329>
- 569 Raichle, M. E., & Mintun, M. A. (2006). Brain work and brain imaging. *Annu Rev Neurosci*, 29,
570 449-476. <https://doi.org/10.1146/annurev.neuro.29.051605.112819>
- 571 RStudio. (2021). *RStudio Team (2021). RStudio: Integrated Development for R.*
572 <http://www.rstudio.com/>. In RStudio.
- 573 Shirer, W. R., Ryali, S., Rykhlevskaia, E., Menon, V., & Greicius, M. D. (2012). Decoding
574 subject-driven cognitive states with whole-brain connectivity patterns. *Cereb Cortex*,
575 22(1), 158-165. <https://doi.org/10.1093/cercor/bhr099>
- 576 Shulman, R. G., Rothman, D. L., Behar, K. L., & Hyder, F. (2004). Energetic basis of brain
577 activity: implications for neuroimaging. *Trends Neurosci*, 27(8), 489-495.
578 <https://doi.org/10.1016/j.tins.2004.06.005>
- 579 Smith, S. M., Fox, P. T., Miller, K. L., Glahn, D. C., Fox, P. M., Mackay, C. E., Filippini, N.,
580 Watkins, K. E., Toro, R., Laird, A. R., & Beckmann, C. F. (2009). Correspondence of the
581 brain's functional architecture during activation and rest. *Proceedings of the*
582 *National Academy of Sciences*, 106(31), 13040-13045.
583 <https://doi.org/10.1073/pnas.0905267106>
- 584 Tabacof, L., Tosto-Mancuso, J., Wood, J., Cortes, M., Kontorovich, A., McCarthy, D., Rizk, D.,
585 Mohammadi, N., Breyman, E., Nasr, L., Kellner, C., & Putrino, D. (2020). Post-acute
586 COVID-19 syndrome negatively impacts health and wellbeing despite less severe
587 acute infection. *medRxiv*, 2020.2011.2004.20226126.
588 <https://doi.org/10.1101/2020.11.04.20226126>
- 589 Taylor, P. A., & Saad, Z. S. (2013). FATCAT: (an efficient) Functional and Tractographic
590 Connectivity Analysis Toolbox. *Brain Connect*, 3(5), 523-535.
591 <https://doi.org/10.1089/brain.2013.0154>

- 592 Tu, Y., Zhang, Y., Li, Y., Zhao, Q., Bi, Y., Lu, X., Kong, Y., Wang, L., Lu, Z., & Hu, L. (2021). Post-
593 traumatic stress symptoms in COVID-19 survivors: a self-report and brain imaging
594 follow-up study. *Molecular Psychiatry*. [https://doi.org/10.1038/s41380-021-01223-](https://doi.org/10.1038/s41380-021-01223-w)
595 [w](https://doi.org/10.1038/s41380-021-01223-w)
- 596 van Schouwenburg, M. R., den Ouden, H. E., & Cools, R. (2015). Selective attentional
597 enhancement and inhibition of fronto-posterior connectivity by the basal ganglia
598 during attention switching. *Cereb Cortex*, 25(6), 1527-1534.
599 <https://doi.org/10.1093/cercor/bht345>
- 600 Wortinger, L. A., Glenne Øie, M., Endestad, T., & Bruun Wyller, V. (2017). Altered right
601 anterior insular connectivity and loss of associated functions in adolescent chronic
602 fatigue syndrome. *PLoS One*, 12(9), e0184325.
603 <https://doi.org/10.1371/journal.pone.0184325>
- 604 Xiao, M., Chen, X., Yi, H., Luo, Y., Yan, Q., Feng, T., He, Q., Lei, X., Qiu, J., & Chen, H. (2021).
605 Stronger functional network connectivity and social support buffer against negative
606 affect during the COVID-19 outbreak and after the pandemic peak. *Neurobiology of*
607 *Stress*, 15, 100418-100418. <https://doi.org/10.1016/j.ynstr.2021.100418>
- 608 Yan, C.-G., Wang, X.-D., Zuo, X.-N., & Zang, Y.-F. (2016). DPABI: Data Processing & Analysis
609 for (Resting-State) Brain Imaging. *Neuroinformatics*, 14(3), 339-351.
610 <https://doi.org/10.1007/s12021-016-9299-4>
- 611 Yeo, B. T., Krienen, F. M., Sepulcre, J., Sabuncu, M. R., Lashkari, D., Hollinshead, M., Roffman,
612 J. L., Smoller, J. W., Zöllei, L., Polimeni, J. R., Fischl, B., Liu, H., & Buckner, R. L. (2011).
613 The organization of the human cerebral cortex estimated by intrinsic functional
614 connectivity. *J Neurophysiol*, 106(3), 1125-1165.
615 <https://doi.org/10.1152/jn.00338.2011>
- 616 Zhang, S., Cui, J., Zhang, Z., Wang, Y., Liu, R., Chen, X., Feng, Y., Zhou, J., Zhou, Y., & Wang, G.
617 (2022). Functional connectivity of amygdala subregions predicts vulnerability to
618 depression following the COVID-19 pandemic. *J Affect Disord*, 297, 421-429.
619 <https://doi.org/10.1016/j.jad.2021.09.107>
- 620
- 621

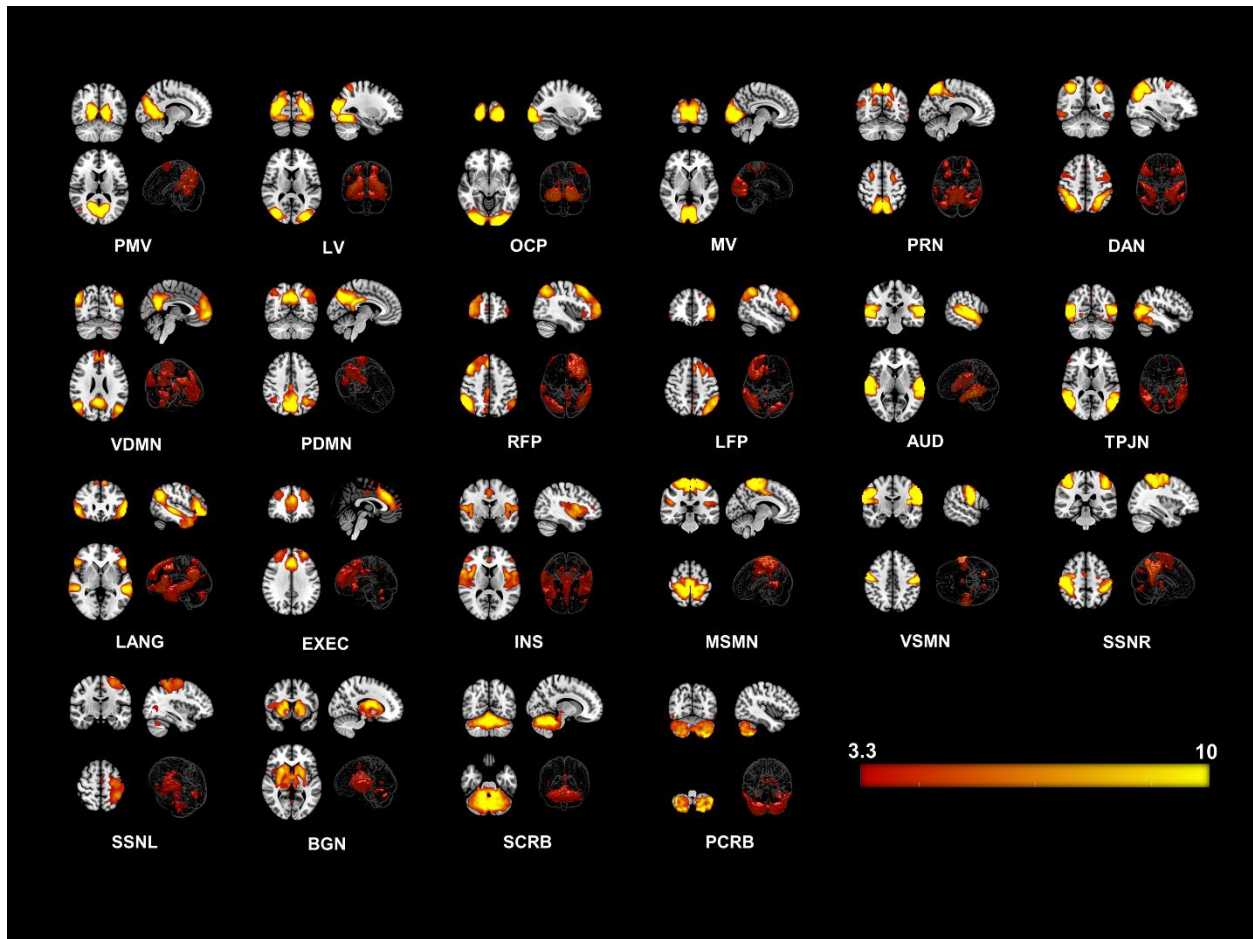


Figure 1. Twenty-two Resting State Networks (RSNs) identified from group ICA using ‘melodic’. Abbreviated names of each network are shown at the bottom of each image. Three orthogonal slices are shown for each network along with a volume rendered image to show depth and three-dimensional view of the RSNs. Statistical estimates (Z-scores) are embedded into a colorbar at the bottom-right. PMV = Primary Visual Network, LV = Lateral Visual, OCP = Occipital Pole, MV = Medial Visual, PRN = Precuneus Network, DAN = Dorsal Attention, VDMN = Ventral Default Mode Network (DMN), PDMN = Posterior DMN, RFP = Right Fronto Parietal, LFP = Left Fronto Parietal, AUD = Auditory, TPJN = Temporo-Parietal Junction Network, LANG = Language Network, EXEC = Executive Control Network, INS = Insular Network, MSMN = Medial Sensory-Motor Network (SMN), VSMN = Ventral SMN, SSNR = Somatosensory Network - Right, SMNL = Somatosensory Network - Left, BGN = Basal Ganglia Network, SCRB = Superior Cerebellar Network, PCRB = Posterior Cerebellar Network.

622

623

624

625

626

627

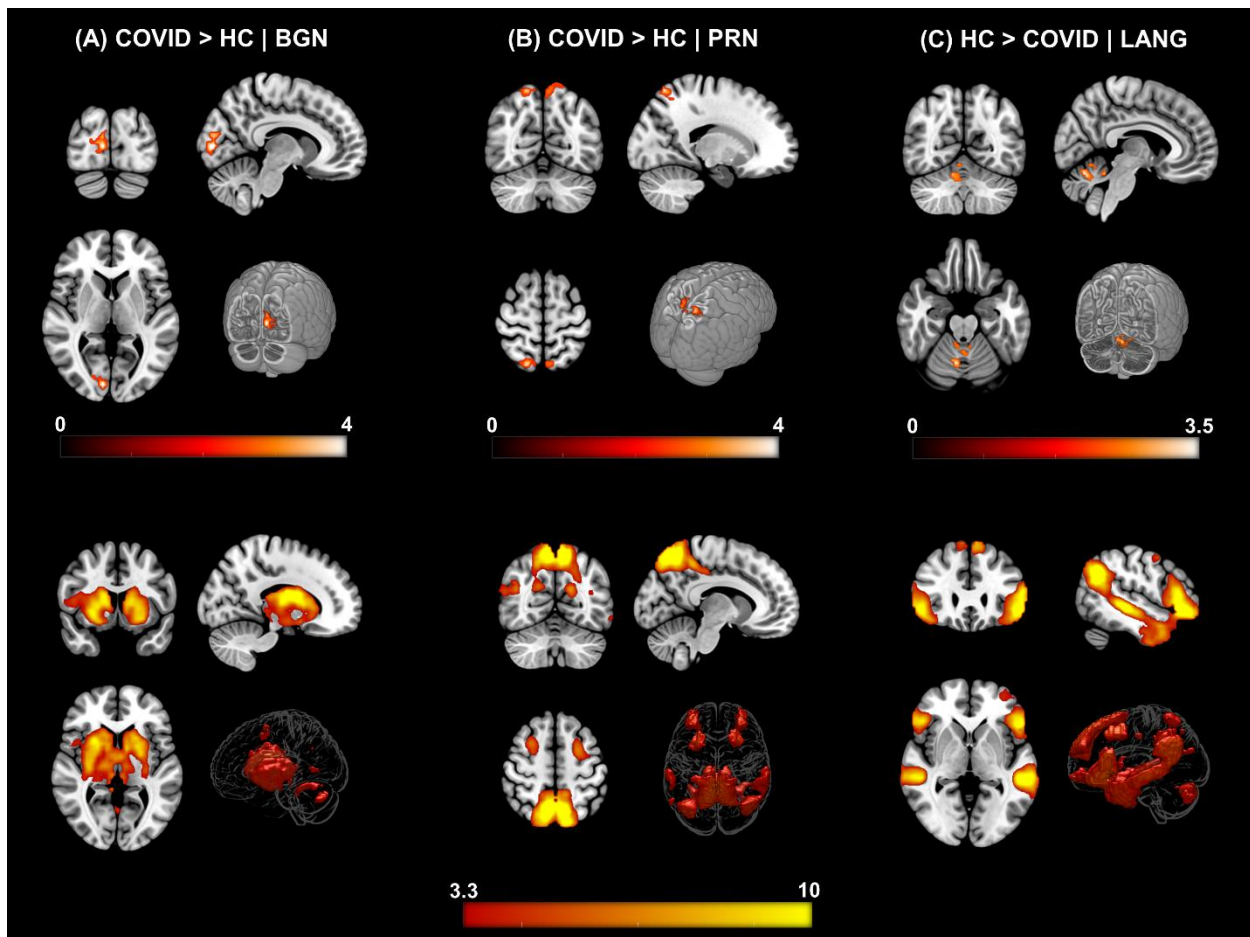


Figure 2. Δ FC | Functional Connectivity differences between COVID survivors and healthy controls. [top row] (A) COVID > HC: Enhanced FC in COVID compared to HCs observed in the *Basal Ganglia Network (BGN)* network. Three orthogonal slices (left) along with a cut-to-depth volume rendered image to show the effects in the *right Calc, Cu* and *LiG*. The colorbar represents t -score values. Cluster information include - cluster peak: $[9 -84 6]$, | cluster extent threshold, $k_E = 69$ | cluster size = 69 voxels. **(B) COVID > HC:** Enhanced FC in COVID compared to HCs observed in the *Precuneus (PRN)* network, demonstrating a significant difference in FC in the *bilateral SPL and PCu* regions. Cluster information include - cluster peak: $[21 -57 54]$, | cluster extent threshold, $k_E = 90$ | cluster size = 90 voxels. **(C) HC > COVID:** Enhanced FC in HCs compared to COVID observed in the *Language (LANG)* network demonstrating significant difference in several vermal layers of the *Cerebellum*. Cluster information include - cluster peak: $[9 -63 -24]$, | cluster extent threshold, $k_E = 57$ | cluster size = 57 voxels. **[bottom row]** Corresponding group level ICA networks from which FC differences are shown on the top row. The colorbar represents z-scores.

628

629

630

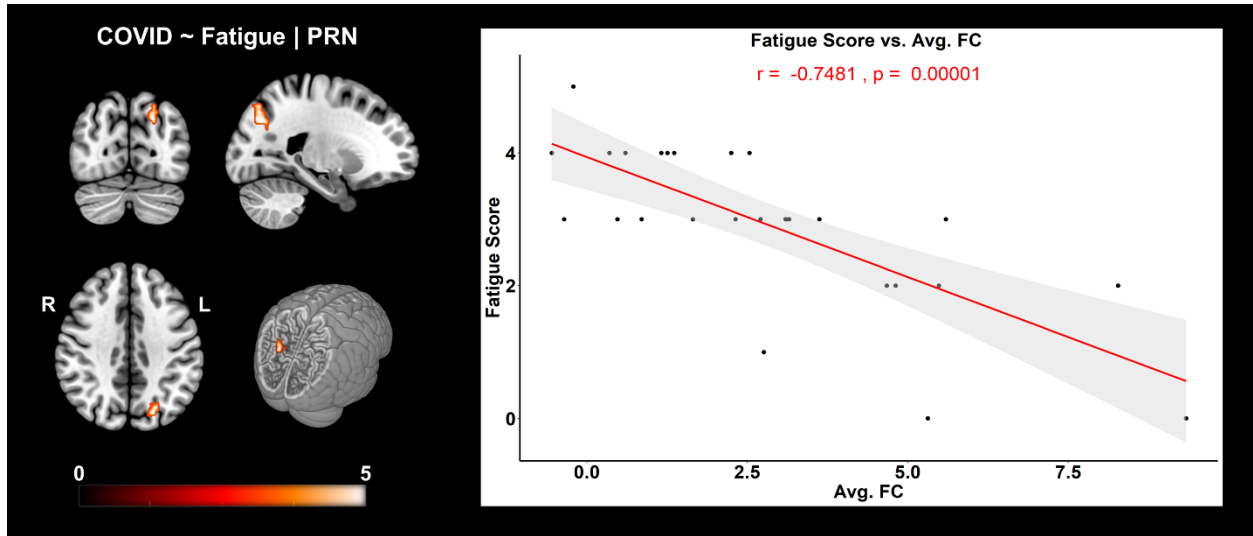


Figure 3. FC corr. Fatigue | COVID: Negative correlation of FC with self-reported fatigue scores in COVID individuals. (left) For the *PRN* network, three orthogonal slices (left) along with a cut-to-depth volume rendered image showing regions from the *Superior Parietal* and *Occipital Gyri* that demonstrated significantly negative correlation with fatigue. The colorbar represents t-score values. **(right)** The graph shows the linear relationship of the average FC within the significant cluster and self-reported fatigue scores from COVID individuals. The x-axis represents the average FC (z-scores) from the cluster and the y-axis represents the fatigue scores. The shaded gray area represents the 95% confidence interval. The red line represents the least squares regression line of best fit. Cluster information include - cluster peak: $[-21 -75 36]$, | cluster extent threshold, $k_E = 58$ and cluster size = 58 voxels.

631

632

633

634

635

636

637

638

Δ FC	RSN Name	Cl. No.	Anatomical Locations	Cl. Ext.	Cl. Size	Peak MNI Coordinates			Peak T, p_{FWE} Values
						X	Y	Z	
COVID > HC	BGN	1	Right – Calcarine Cortex (<i>Calc</i>)	69	69	9	-84	6	4.46, 0.004
			Right – Cuneus (<i>Cun</i>)						
			Right – Lingual Gyrus (<i>LiG</i>)						
	PRN	1	Right – Superior Parietal Lobule (<i>SPL</i>)	90	90	21	-57	54	4.22, 0.001
			Right – Precuneus (<i>PCu</i>)						
			Left – Superior Parietal Lobule (<i>SPL</i>)						
Left – Precuneus (<i>PCu</i>)									
HC > COVID	LANG	1	Right – Cerebellar Exterior (<i>CExt.</i>)	57	57	9	-63	-24	3.56, 0.019
			Right – Cerebellar Vermal Lobules I-V						
			Right – Cerebellar Vermal Lobules VI-VII						

Table 1. List of spatial regions from significant clusters obtained from the contrast – COVID > HC. The regions from three RSNs – *BGN*, *PRN* and *LANG* which demonstrated significant differences are presented with peak MNI coordinates (X Y Z) and corresponding peak t-score values for each cluster. Keys – Δ FC = Direction of change in Functional Connectivity; Cl. = Cluster; Cl. No. = Cluster Number; Cl. Ext. = Cluster Extent Threshold; Cl. Size = Cluster Size; T = peak t-score; p_{FWE} = corrected p-value.

639

640

641

Corr (FC, ftg.)	RSN Name	Cl. No.	Anatomical Locations	Cl. Ext.	Cl. Size	Peak MNI Coordinates			Peak T, p_{FWE} Values
						X	Y	Z	
COVID	PRN	1	Left – Superior Parietal Lobule (SPL)	58	58	-21	-75	36	5.31, 0.01
			Left – Superior Occipital Gyrus (SOG)						
			Left – Angular Gyrus (AnG)						
			Left – Precuneus (PCu)						

Table 2. List of spatial regions from clusters showing significant correlation with self-reported fatigue among COVID individuals. The regions from PRN which demonstrated significant correlation are presented with peak MNI coordinates (X Y Z) and corresponding peak t-score values for each cluster. Keys – FC = Functional Connectivity; ftg. = Fatigue Scores, Cl. = Cluster; Cl. No. = Cluster Number; Cl. Ext. = Cluster Extent Threshold; Cl. Size = Cluster Size; T = peak t-score; p_{FWE} = corrected p-value.

642

643